SYSTEMS, SCIENCE AND SOFTWARE

SSS-R-77-3019

A STUDY OF COMPOSITE MATERIAL DAMAGE INDUCED BY LASER-SUPPORTED DETONATION WAVES

FINAL REPORT

J. R. TRIPLETT
G. A. GURTMAN

CONTRACT N00014-75-C-0993

OFFICE OF NAVAL RESEARCH
ARLINGTON, VIRGINIA

SEPTEMBER 1976

P. O. BOX 1620, LA JOLLA, CALIFORNIA 92038, TELEPHONE (714) 453-0060

SYSTEMS, SCIENCE AND SOFTWARE

SSS-R-77-3019

A STUDY OF COMPOSITE MATERIAL DAMAGE INDUCED BY LASER-SUPPORTED DETONATION WAVES

FINAL REPORT

J. R. TRIPLETT
G. A. GURTMAN

CONTRACT N00014-75-C-0993

OFFICE OF NAVAL RESEARCH
ARLINGTON, VIRGINIA

SEPTEMBER 1976

P.O. BOX 1620, LA JOLLA, CALIFORNIA 92037, TELEPHONE (714) 453-0060

UNCLASSIFIED

SECURITY CLASSIFICATION OF THIS PAGE (When Data Entered)

REPORT DOCUMENTATION PAGE	READ INSTRUCTIONS BEFORE COMPLETING FORM
1. REPORT NUMBER (9) Final rept. 2. GOVT ACCESSION NO.	3. RECIPIENT'S CATALOG NUMBER 1 Apr 75 - 30 Sep 76
4. TITLE (and Subtitle) (6) A Study of Composite Material Damage Induced by Laser-Supported Detonation Waves	5. TYPE OF REPORT & PERIOD COVERED Final Report 4/1/75 - 9/30/76
(14)	6. PERFORMING ORG. REPORT NUMBER SSS-R-77-3019
7. AUTHOR(s) (10) J. R. Triplett G. A. Gurtman	8. CONTRACT OR GRANT NUMBER(s) (15) N00014-75-C-0993
9. PERFORMING ORGANIZATION NAME AND ADDRESS Systems, Science and Software P. O. Box 1620 La Jolla, California 92038	10. PROGRAM ELEMENT, PROJECT, TASK AREA & WORK UNIT NUMBERS NR 064-569
11. CONTROLLING OFFICE NAME AND ADDRESS Department of the Navy Office of Naval Research Arlington, Virginia 22217	(11) Sep [redacted] 76 13. NUMBER OF PAGES 30 (12) 34pg
14. MONITORING AGENCY NAME & ADDRESS(if different from Controlling Office)	15. SECURITY CLASS. (of this report) Unclassified
	15a. DECLASSIFICATION/DOWNGRADING SCHEDULE

16. DISTRIBUTION STATEMENT (of this Report)

DISTRIBUTION STATEMENT A
Approved for public release;
Distribution Unlimited

17. DISTRIBUTION STATEMENT (of the abstract entered in Block 20, if different from Report)

18. SUPPLEMENTARY NOTES

19. KEY WORDS (Continue on reverse side if necessary and identify by block number)

LSD waves
Composite material damage
Ductile fracture
Stress wave propagation

20. ABSTRACT (Continue on reverse side if necessary and identify by block number) cm SQUARE

A model for ductile fracture is applied to the analysis of failure modes on a carbon-phenolic composite, loaded at the surface by a laser-supported detonation wave. It is demonstrated that for a 100 joule/cm², 10 ns pulse the model predicts failure of the sample as the third reflected tensile stress wave propagates through it. It is argued that high-intensity, short pulses are capable of producing damage

388 507

DD FORM 1 JAN 73 1473 EDITION OF 1 NOV 65 IS OBSOLETE

UNCLASSIFIED

SECURITY CLASSIFICATION OF THIS PAGE (When Data Entered)

20. ABSTRACT (cont'd)

efficiently in composites, but that with LSD surface loading rather than direct laser-target interaction the rapid stress relief required for front-surface spall failure is difficult to achieve. The attenuation of stress waves in the composite due to dispersion and viscous dissipation, the effects of defects in the virgin material, and the nucleation and growth parameters for cracks in different composite materials are critical factors in the analysis.

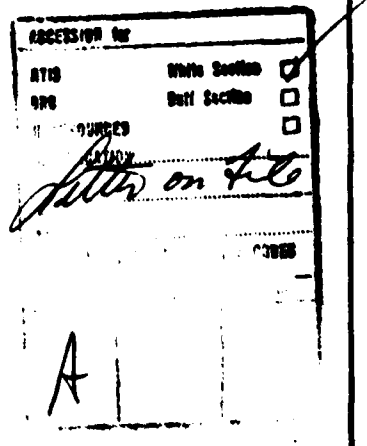

TABLE OF CONTENTS

LIST OF ILLUSTRATIONS

1. INTRODUCTION

The general objective of the research described in this report is to understand how composite materials may be damaged by the surface stress loading resulting from the ignition of laser-supported detonation (LSD) waves in the atmosphere adjacent to the surface. This type of surface loading is distinguished from others (flyer plate, x-ray, electron beam, direct laser-target interaction) by the relatively weak mechanical coupling between the region in which the stress is created and the bulk of the target material. This results both from the mismatch in mechanical impedance between the air and the solid target, and from the physical separation of the air shock and the solid surface. As a result of this weak coupling, the peak stress developed in the target for a given energy input is comparatively low. Furthermore, the stress relief at the surface tends to be relatively slow, but a large total impulse may be transferred to the target over an extended period of time at very low stress levels.[1]

These features of the LSD-target interaction imply that simple empirical damage criteria developed to correlate experimental results obtained with other types of loading may not be useful for the LSD case. We have therefore employed a more complex criterion, essentially that developed at Stanford Research Institute (SRI) for ductile fracture,[2] which is based on detailed models of the nucleation and growth of defects, together with a large number of microscopic measurements.

---

1. Schriempf, J. T., "Response of Materials to Laser Radiation," NRL Report 7728, 1974.

2. Seaman, L., T. W. Barbee, Jr. and D. R. Curran, "Dynamic Fracture Criteria of Homogeneous Materials," Air Force Weapons Laboratory Report AFWL-TR-71-156, 1971.

In the absence of direct results on LSD-induced damage in composites, this approach appears to be more realistic than the simple maximum-stress, total-impulse or strain-energy models employed previously.

The general features of the LSD-composite interaction outlined above also have implications for the characteristics of the laser beams which may be expected to induce significant damage. For a given fluence incident on the target, say 100 joules/cm^2, one increases impulse by reducing the intensity (lengthening the pulse time) but increases peak stress by increasing the intensity (shortening the pulse). Both the strain-energy and SRI damage criteria, in a general way, are more dependent on peak stress than on impulse. The predicted damage, for moderate fluences at least, has a threshold at some minimum intensity, and increases with intensity above this level.

There are upper limits on both intensity and fluence for laser beam propagation through the atmosphere, which depend on the wavelength of the laser, the number and size of aerosol particles in the air, the time profile and optical characteristics of the laser pulse, and the propagation distance between the laser and the target. Here it will merely be remarked that intensity alone is not a proper criterion for propagation of pulsed laser beams and in fact for pulses shorter than 10 ns the limit is more accurately expressed in terms of fluence. For sufficiently low fluences, i.e., short pulses, instantaneous intensities well above the continuous-wave (C-W) breakdown threshold for intensity can be propagated; one measurement[3] yielded a threshold of 800 joules/cm^2 for a 0.02 ns neodymium laser pulse. The corresponding intensity is over 100 times the C-W breakdown threshold, an extreme

---

3. Ireland, C. L. M., A. Yi, J. M. Aaron, and C. Grey Morgan, "Focal-Length Dependence of Air Breakdown by a 20-psec Laser Pulse," Appl. Phys. Letter 24, 175, 1974.

case. Above about 10^{12} watts/cm^2, of course, nonlinear-optics phenomena may occur which provide a genuine intensity limit for air propagation, but surface stresses of several kilobars can be achieved for intensities well below that.

Multiple-pulse laser systems provide, in principle, the capability of delivering high total fluences to the target without sacrificing the intensity and peak stress conditions needed for inducing damage. There are a number of problems in the multiple-pulse systems which require study, but we have chosen to consider first the mechanical characteristics of the composite target which provide the basis for any evaluation of laser system requirements. In particular, answers are needed to questions such as the following:

1. Under what conditions, if any, can front-surface tension be produced by LSD-wave loading?
2. Under what conditions can damage be induced by shear loading, as for example at the edge of the irradiated spot?
3. What front-surface loading conditions are required to produce a reflected tension wave from the back surface of a target capable of producing damage?
4. How are the damage characteristics of a composite related to the composition, structure, porosity, etc. of the material?
5. Assuming that the damage process is initiated, under what conditions will the target proceed to complete fracture?

The work described below is a first step only toward the resolution of some of these questions (in particular the last three). It is believed that further progress along these lines may result in a much improved insight into the laser-composite interaction, and provide a valuable guide to future experimental and theoretical efforts.

Section 2 contains a description of the ductile fracture model. Sections 3 and 4 discuss the material equation of state and the artificial viscosity model used in the calculations, which in turn are described in Section 5. Some conclusions are discussed in Section 6.

2. MODEL FOR DUCTILE FRACTURE

The ductile fracture model we have employed is a modified version of that of L. Seaman, et. al.[2] In the SRI ductile fracture model, nucleation of cracks occur at a rate

$$\dot{N} = \dot{N}_o \exp \frac{\sigma - \sigma_{no}}{\sigma_1}$$

if the ambient tensile stress σ exceeds a threshold σ_{no} (otherwise $\dot{N} = 0$). Similarly, cracks already present grow at a rate

$$\dot{R} = \frac{\sigma - \sigma_{go}}{4\eta} \quad R$$

if σ exceeds a threshold σ_{go}, where R is the crack radius. The following constants are given for two-dimensional carbon phenolic composites.[4]

$\sigma_{no} = 0.2$ kbar

$\dot{N}_o = 2.1 \times 10^{10}$ cm^3/sec

$R_o = 5 \times 10^{-3}$ cm

$\sigma_1 = 0.38$ kbar

$\sigma_{go} = 0$

$\eta = 89.3$ dyne-sec/cm^2

In our implementation of this model, the radius R is replaced by the fractional void volume $V \sim N R^3$. The ambient stress σ is related to V by the linear relation

---

4. Shockey, D. A., L. Seaman, M. Austin, D. R. Curran, and R. A. Armistead (Stanford Research Institute), "Repetitively Pulsed Laser Induced Fracture as a Damage Enhancement Mechanism," Proceedings of the 1975 DOD Laser Effects/Hardening Conference, NASA TM X-73,084, Vol. II, p. 373.

$$\sigma = \sigma_s \ (1 - \alpha_c V) \tag{1}$$

where α_c is a constant taken[2] to be 2.0 and σ_s, the stress in the solid, is assumed to be independent of V and can be evaluated at the beginning of each step from the known value of σ and V. A second relation between σ and V is the differential equation

$$\frac{dV}{dt} = \dot{V}_o \exp\left(\frac{\sigma - \sigma_{no}}{\sigma_1}\right) + \frac{3}{4\eta} \ (\sigma - \sigma_{go}) \ V \tag{2}$$

where $\dot{V}_o \sim \dot{N}_o R_o^3$. This equation states that the total change in fractional void volume results from the production of new void nuclei and from the growth of voids already present. Since this equation is linear in V, its analytic solution may be used together with (1) in an iterative root-finding procedure which determines a time-advanced value of V and a corresponding modified value of σ. Since the terms on the right side of (2) cannot be negative, the procedure can only increase the void volume and decrease the ambient tensile stress. When V for any mass element exceeds the value $0.95/\alpha_c$ a fracture flag is set. In this calculation, the fractured region was treated as essentially void, able to reflect both tension and compression waves.

3. EQUATIONS OF STATE

The equations of state for the fiber and resin constituents are described in detail in Reference 5. A brief summary is presented below. The Mie-Gruneisen form

$$P = G\rho E + (1 - \frac{1}{2} G\mu)\ P_H\ (\mu)$$

is assumed for $\rho > \rho_o$ (compressed materials) where P is the pressure, G the Gruneisen coefficient, E the specific internal energy,

$$\mu = \frac{\rho}{\rho_o} - 1$$

and $P_H\ (\mu)$ is the Hugoniot pressure. For carbon fibers, with $\rho_o = 1.59$, the Hugoniot is represented by:

$$P_H = 73.6\ \mu\ \text{(kbar)}, \qquad 0 < \mu < 0.3$$

$$= 71.58 - 403.62\ \mu + 795.37\ \mu^2\ \text{(kbar)}, \qquad \mu > 0.3$$

The Gruneisen coefficient for carbon fibers is assumed to vary with E. With

$$\Gamma = 0.24 \qquad E < 7.247\ \text{kJ/g}$$

$$= 0.667 \qquad E > 66.24\ \text{kJ/g}$$

---

5. Gurtman, G. A., M. H. Rice, R. A. Cecil and E. W. Sims, "Material Response Models for Radiation Effects on Advanced Three-Dimensional Composite Heat Shield Materials," Air Force Weapons Laboratory Report AFWL-TR-74-144, 1975.

and interpolated linear dependence on energy for intermediate values of E, then

$$G(E) = \frac{\rho_o}{\rho E} \int_o^E \Gamma dE$$

defines the Gruneisen coefficient for carbon fibers.

For phenolic resin, with $\rho_o = 1.25$ and $\rho > \rho_o$,

$$P_H = 69.6\ \mu + 615\ \mu^2 - 839\ \mu^3 + 656\ \mu^4 \quad \text{(kbar)}$$

and

$$G = G(\rho) = \frac{\rho_o}{\rho} [0.52 + 0.68\ \mu \exp(-1.238\ \mu)] \quad .$$

For expanded materials, with $\rho < \rho_o$, let

$$\varepsilon = 1 - \frac{\rho_o}{\rho}$$

be the "engineering" strain variable. Then the pressure is assumed in the form

$$P = G\rho\ [E - E_s(E)\ (1 - \exp(N \frac{\rho_o}{\rho} \varepsilon))]$$

with

$$N = \frac{K_o}{\rho_o G_o E_s(E)}$$

where K_o and G_o are the bulk modulus and Gruneisen coefficients at $\rho = \rho_o$.

For carbon fibers with $\rho < \rho_o$,

$$G = G(E)\ [1 + \epsilon \exp\ (-\frac{\epsilon}{10})]$$

where G(E) is defined as above for compressed carbon fibers. The sublimation energy for carbon fibers is taken as

$$E_s(E) = 7.247 \text{ kJ/g}, \qquad E < 7.247 \text{ kJ/g}$$
$$= 58.99 \text{ kJ/g}, \qquad E > 66.24 \text{ kJ/g}$$

with linear dependence on E for intermediate values.

For phenolic resin, with $\rho < \rho_o$

$$G = G(\rho) = 0.20 + 0.32\ \sqrt{\rho/\rho_o}$$

and

$$E_s(E) = 836.8 \text{ (joule/g)} \qquad E < 836.8 \text{ joule/g}$$
$$= \frac{2}{3}\ (E - 836.8) + 836.8 \qquad 836.8 < E < 3033.4$$
$$= 2301.2 \qquad E > 3033.4$$

For composites with fibers perpendicular to the direction of propagation, the shear modulus and yield strength are assumed zero. The fiber and resin constituents of each cell are equilibrated mechanically and thermally; the total energy and volume of a cell is divided between fiber and resin so as to yield the same pressure and temperature. The composite is assumed to be 59.34 percent fiber and 40.66 percent resin, by volume, for the perpendicular fiber orientation, with zero initial porosity.

4. ARTIFICIAL VISCOSITY MODEL

Many finite-difference calculations of stress-waves employ a quadratic artificial viscosity

$$q_1 = -k_1 \rho |\Delta u| \Delta u, \quad \Delta u < 0$$

for numerical stabilization of strong shocks, plus a linear term

$$q_2 = -k_2 \rho c \, \Delta u$$

for elastic solids, where ρ is the density, Δu the velocity increase across a zone, and c the sound speed, with k_1, k_2 being dimensionless coefficients. The quadratic term q_1 is always switched off for expanding zones, but the linear term may be used in expansion, compression or both. The linear term q_2 is useful for stabilizing the numerical calculation for weak shocks in solids, since the q_1 term is too small to be effective for these materials. However, the q_2 viscosity is dissipative and may attenuate narrow stress pulses.

A quadratic formulation of artificial viscosity for elastic solids[6] was therefore introduced:

$$q_3 = -k_3 \, (\Delta p)^2 / \overline{p}$$

$$= -k_3 \, \Delta u \, \left| \Delta u \cdot \frac{\Delta p}{\Delta E} \right| , \quad \Delta u > 0$$

---

6. White, J. W., "A New Form of Artificial Viscosity for Elastic Solids," J. Comp. Phys. 16, 119-126, 1974.

where $\bar{p}$ is the mean pressure in the shock, and the second form may be obtained by using the second and third Rankine-Hugoniot relations. The ratio $\Delta p/\Delta E$ was evaluated as

$$\frac{dP}{dt} / \frac{dE}{dt}$$

using single-step time differencing. The term was used only for expanding zones. In the calculation described later in this report, it was successful in calculating the initial compressive pulse propagation with much less attenuation than occurred with q_2, but failed to allow a stable reflection from the back surface of the composite layer. The calculation was therefore continued from this stage with q_1 and q_2 terms only. The instability of the q_3 model at the back surface is not at this point fully understood, but it should be noted that the model was developed for homogeneous materials with simple elasticity rather than for the more complex material in our application.

The spreading of the wave profiles resulting from the q_2 formulation is too severe to be totally ignored. While in the present series of calculations the energy dissipation due to q_2 is numerical in nature, it should be noted that most polymeric materials (such as phenolic) are somewhat viscous. This time dependence is not currently accounted for in our rather simple solid equation of state for phenolic (see Section 3). The calculated pulse spreading and resultant attenuation might therefore be a reasonable approximation to 2DCP constitutive behavior, but it would be necessary to compare numerical results with experimentally determined wave profiles to ascertain this to with any degree of confidence. We might note also that the geometric (and non-dissipative) dispersion inherent in any laminated composite made up of constituents possessing differing shock impedances, is correctly modeled in the existing code formulation.

5. CALCULATION RESULTS

The prototype calculation here presented is intended to exhibit the performance of the ductile fracture model and the other analytic techniques which have been developed for the study of laser-composite interactions. Additional calculations of this type would be required in order to infer actual failure criteria for the material represented, since the parameters of the calculation were purposely chosen to be relatively favorable to the production of damage.

The target material, a two-dimensional carbon-phenolic composite, was described in Section 3 above. The thickness of the sample was 0.254 cm (100 mils). The incident laser pulse fluence was 100 joules/cm^2 and the total pulse time 10 ns. The arbitrarily chosen pulse shape (shown in Figure 1) and wavelength (1.06 μm) had very little effect on the calculation; the neodymium wavelength was used since a CO_2 laser pulse with this fluence and length would not propagate through clean air. The reflectivity of the surface was unity, and the density of LSD wave nucleation sites 10^4/cm^2. The absorption of laser radiation in the LSD wave was represented by the model described in Reference 7. One-dimensional propagation was assumed, so that no lateral rarefactions contributed to the stress relaxation at the surface following the pulse.

Figure 1 shows the peak pressure in the LSD wave for the first 10 ns and the ensuing blast wave for an additional 15 ns. Figure 2 shows the pressure in the air adjacent to the solid surface for the same initial 25 ns. The maximum at 15 ns represents the arrival of the blast wave resulting from the cutoff of the laser pulse. The surface air pressure is also shown

---

7. Triplett, J. R., and R. A. Cecil, "A Study of Laser-Supported Detonation Wave Interactions with Three-Dimensional Composites," Systems, Science and Software Report SSS-R-76-2743, 1 October 1975.

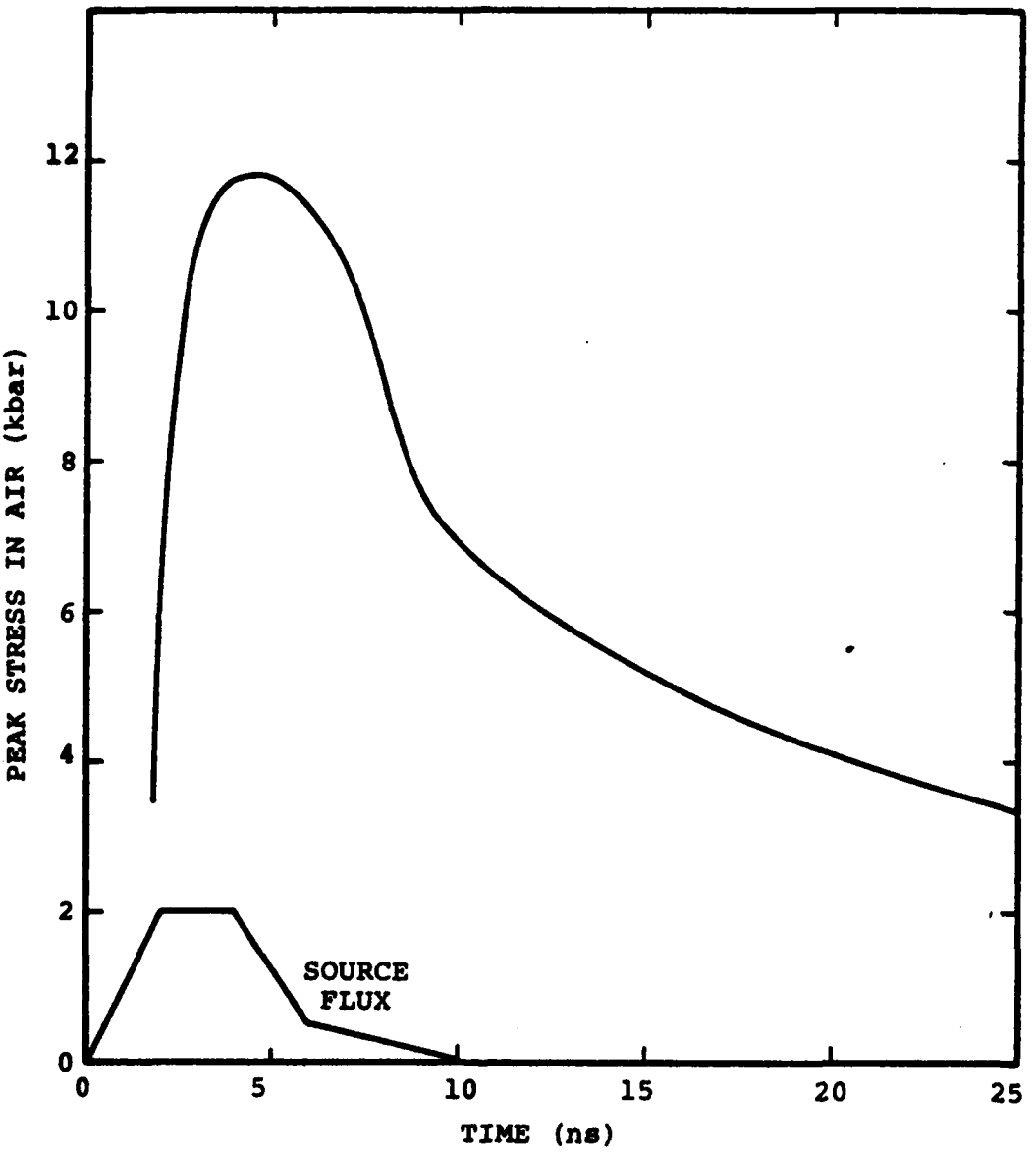

Figure 1. Peak stress in air shock versus time.

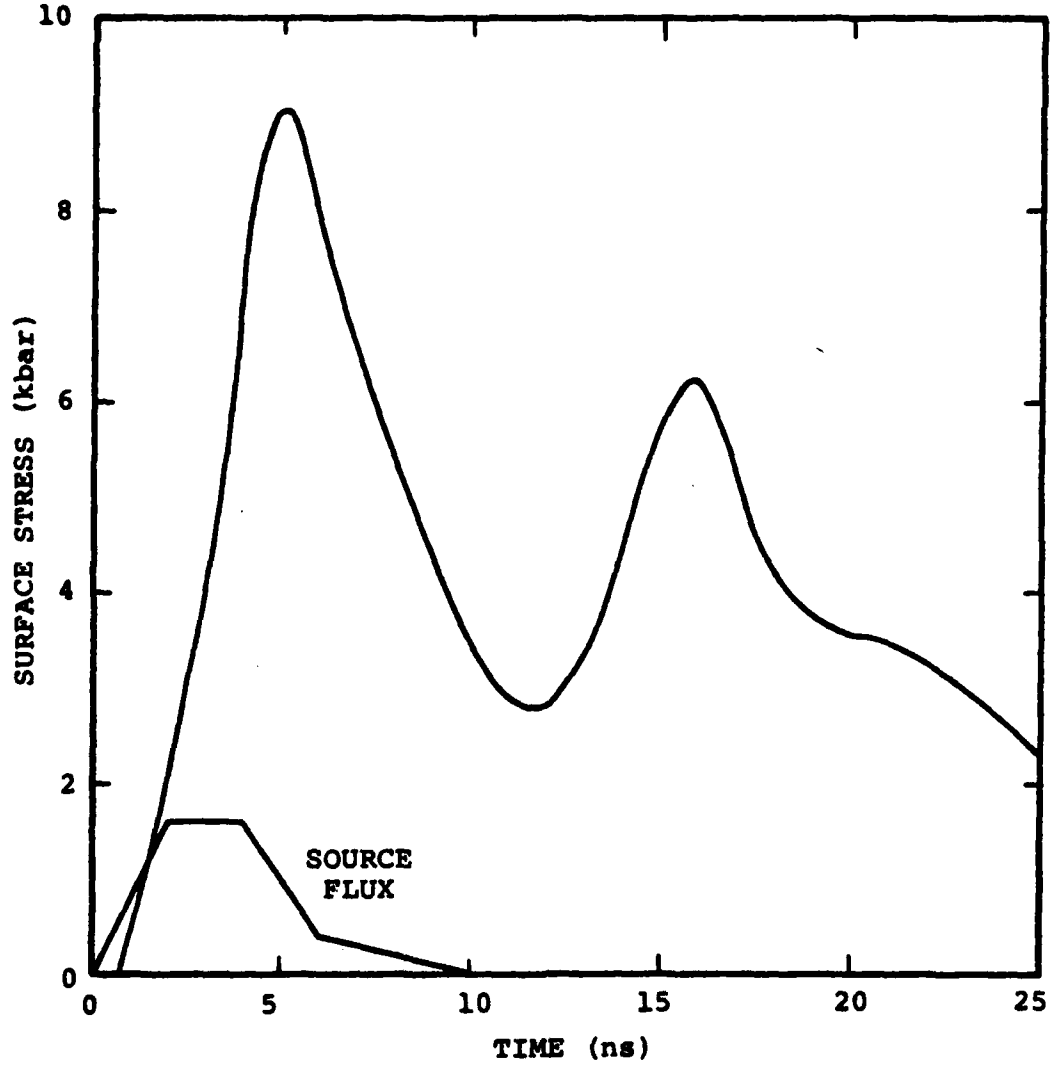

Figure 2. Surface stress in air versus time.

in Figure 3 on a longer time scale, to 1.2 μs. This very gradual relaxation effectively prevented any tensile stresses from developing near the front surface. In a real situation, lateral rarefactions and radiative cooling would provide a more rapid relief of the front-surface stress, at least at late times.

Figure 4 shows the wave loci and damage contours on a space-time diagram, with compressive waves shown as broken lines. The first tension wave produces most of the microcracks, but is incapable of driving them to significant size. The contour for 10^{-3} void volume fraction coincides with this wave through most of the composite, excluding only thin layers near the front and back surfaces. The second tension wave brings the void fraction to order 10^{-1} throughout the central two-thirds of the target. The curvature of the wave locus results from the attenuation of the wave, here in a nonlinear portion of the Hugoniot.

The third tension wave initiates the fracture locus at a point about 75 percent through the target, at time 4.25 us. From this point on, the waves reverberate between the fracture boundary and the surfaces of the target.

The damage contours expand under tensile stress only, so are somewhat irregular. At 8 μs the fractured region occupies most of the interior of the layer and is still expanding slowly.

Figure 5 shows the peak stress in the first and second waves. The remaining figures are plots of the spatial wave shapes. Figure 6 shows the first compression wave, Figures 7 and 8 the first tension wave. Figures 9 and 10 show the second wave and Figure 11 the third compression wave. In Figure 12 the third tension wave has just been interrupted by the fracture of the material, and the two sections have reflected as separate compression waves in Figure 13.

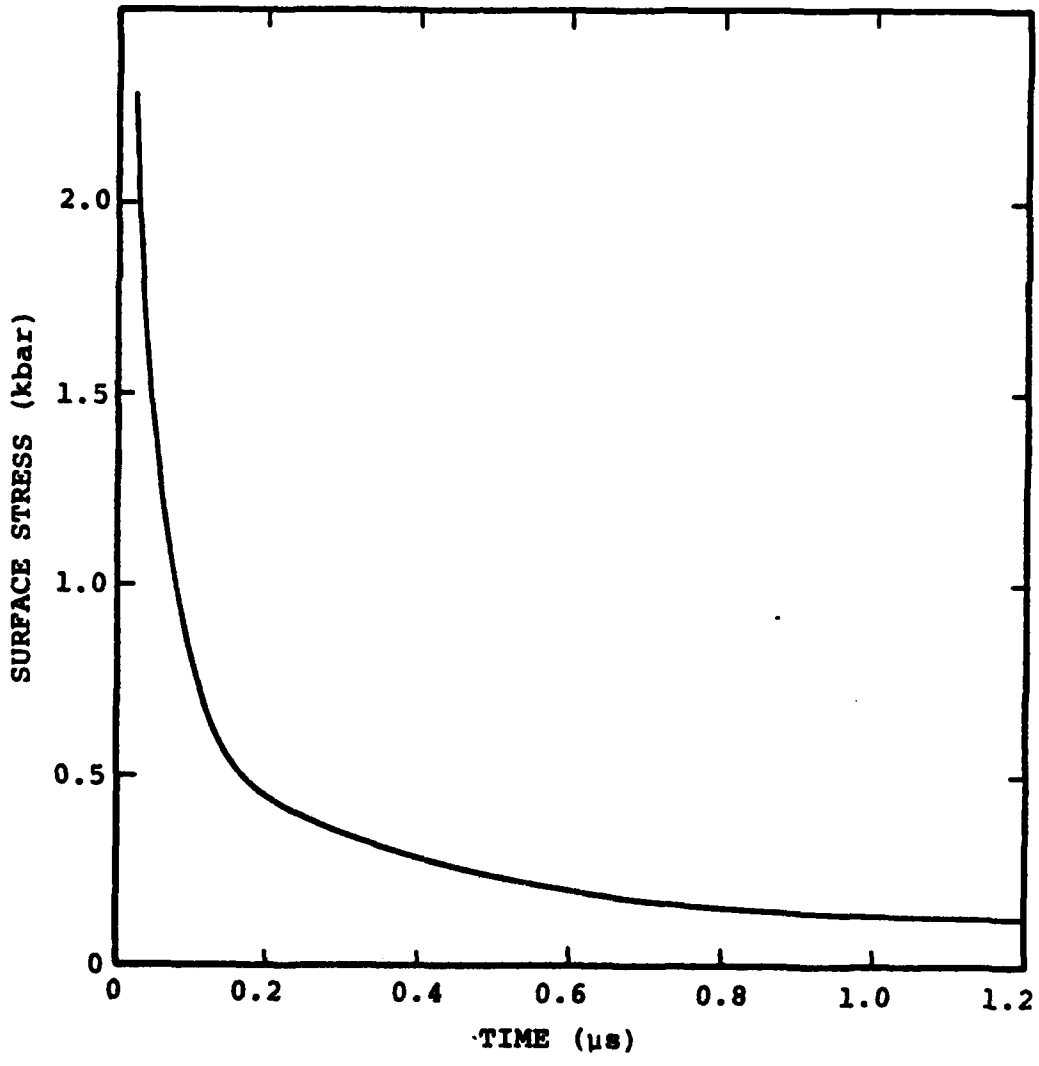

Figure 3. Surface stress in air versus time.

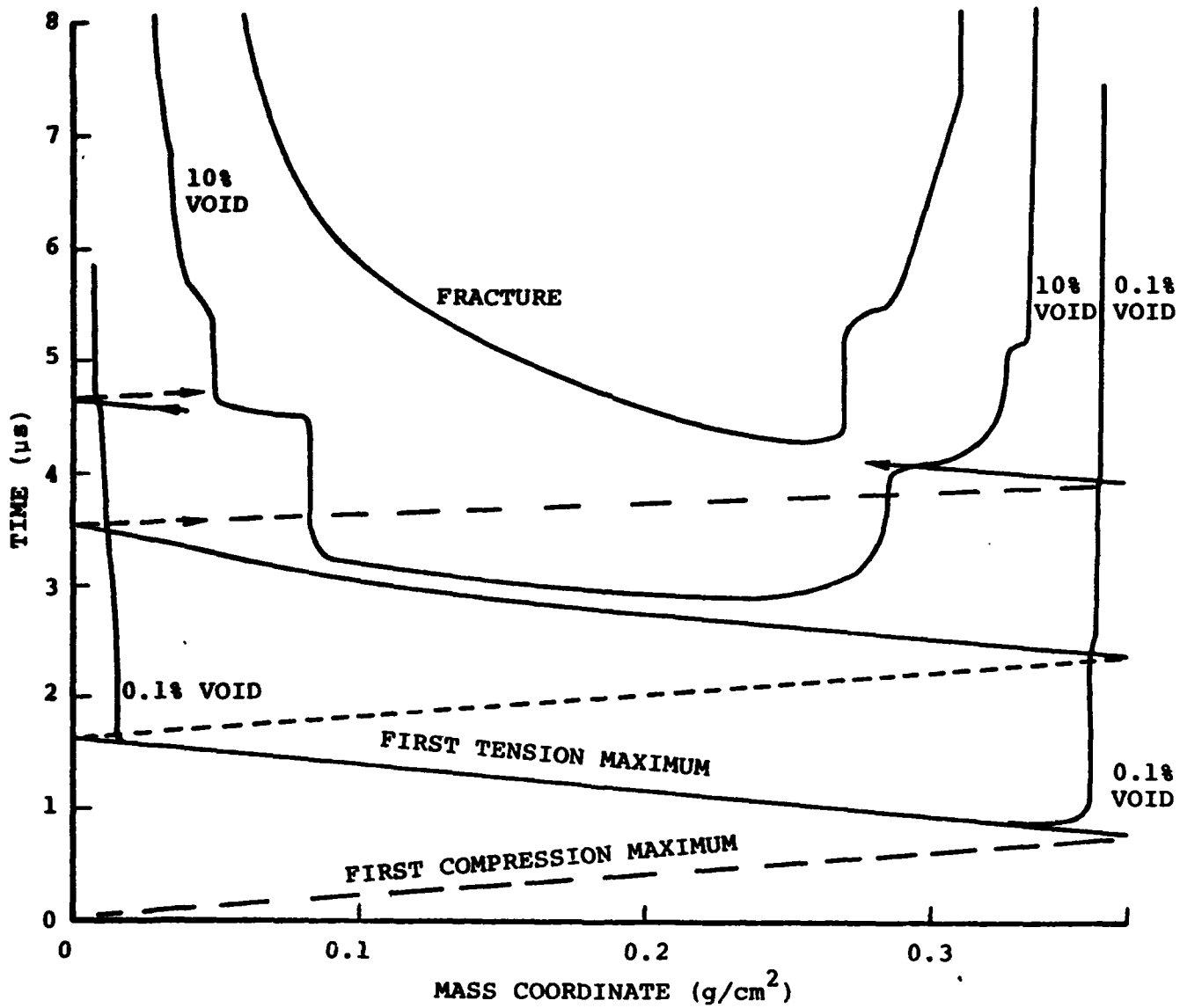

Figure 4. Wave loci and damage contours.

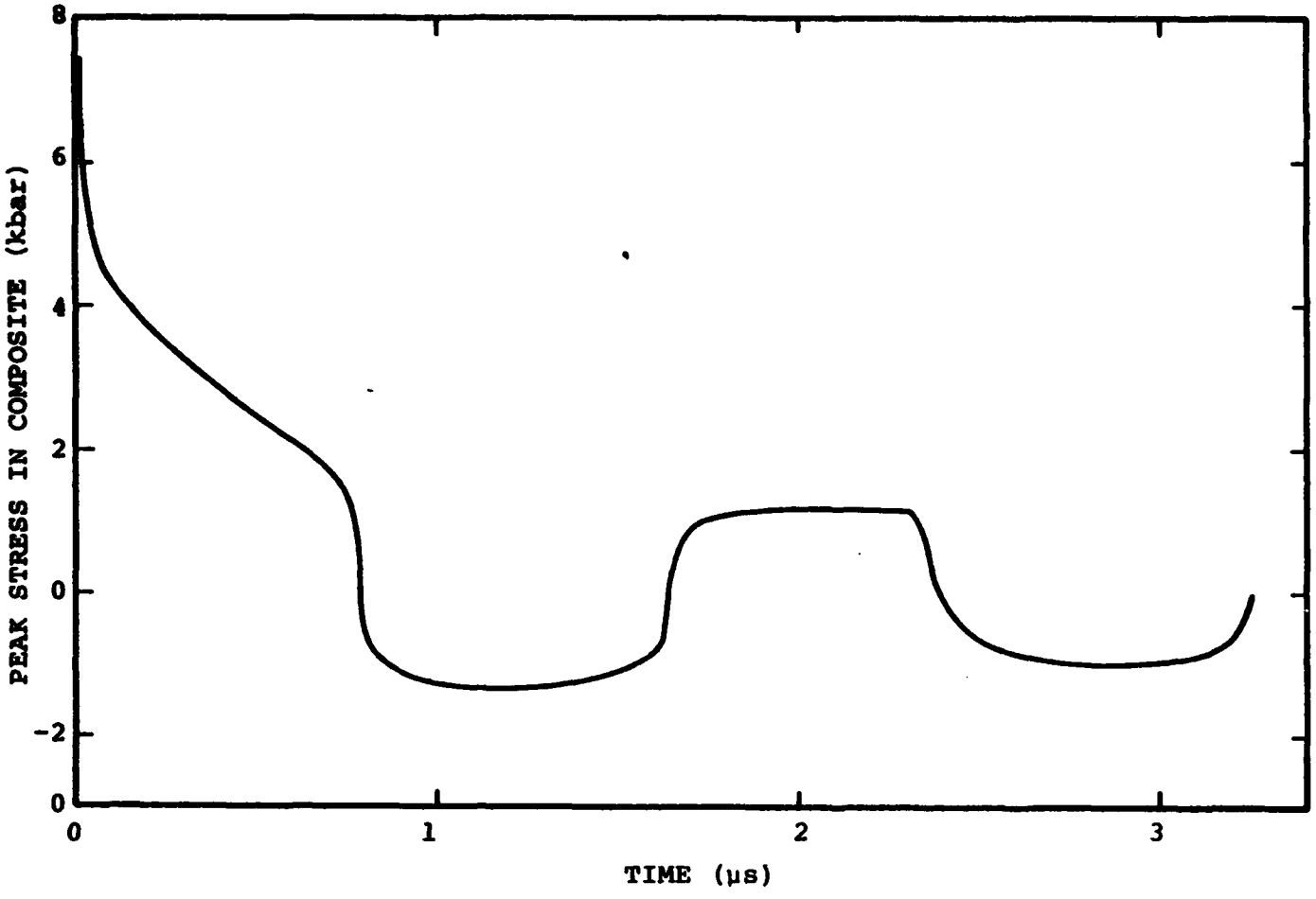

Figure 5. Peak stress in composite versus time.

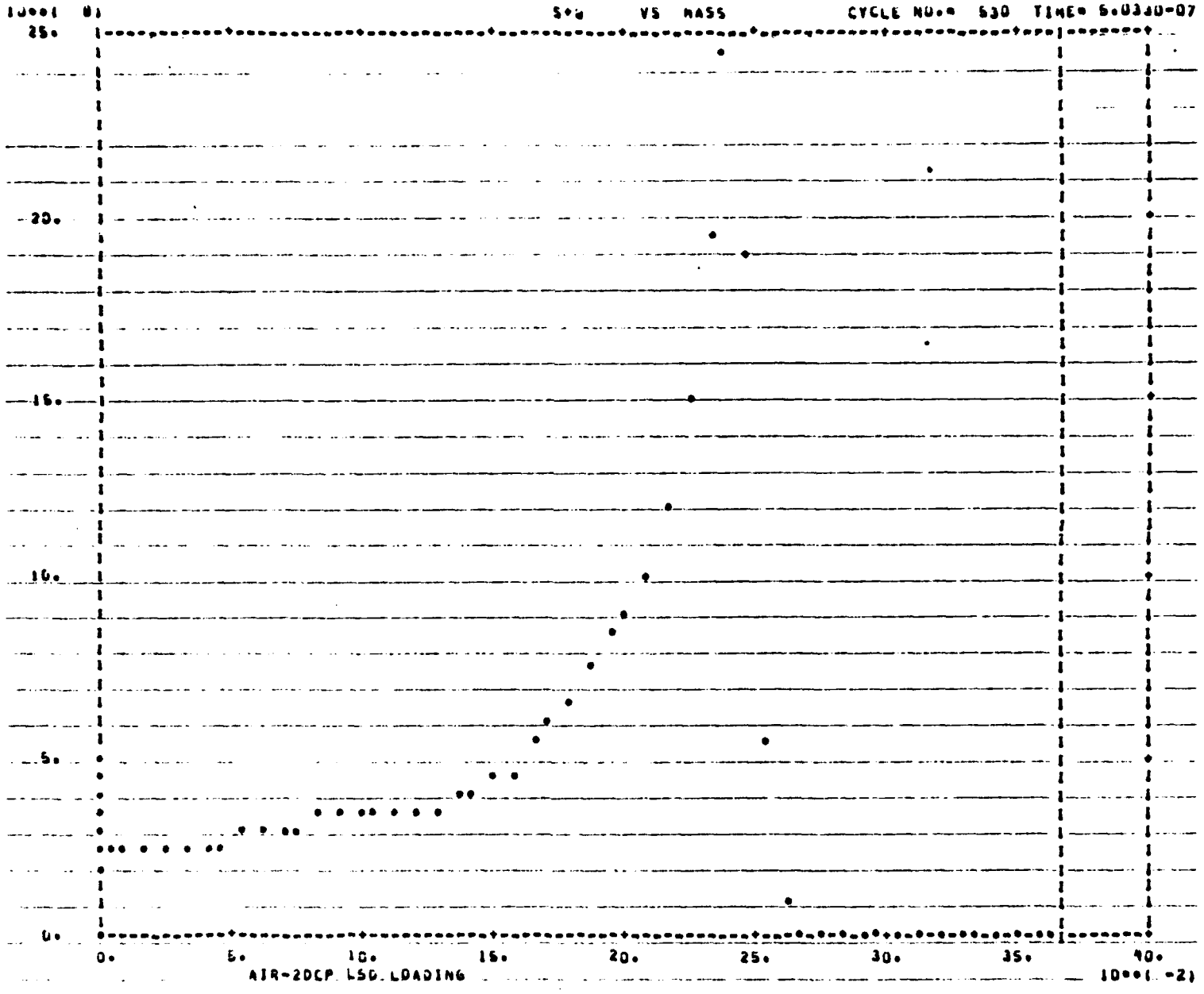

Figure 6. Stress (dynes/cm^2) versus mass depth (g/cm^2) at 0.50 μs.

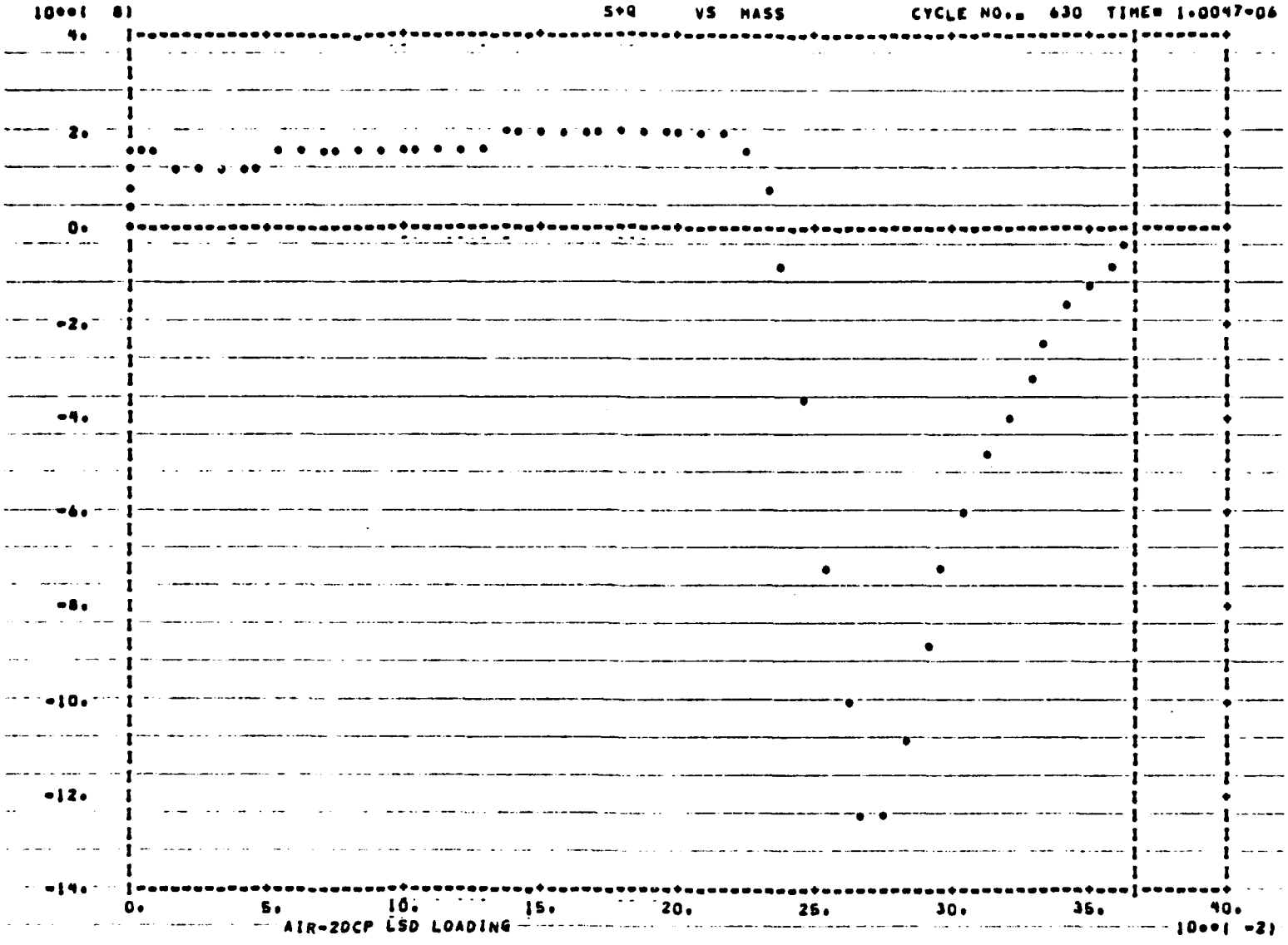

Figure 7. Stress (dynes/cm^2) versus mass depth (g/cm^2) at 1.00 μs.

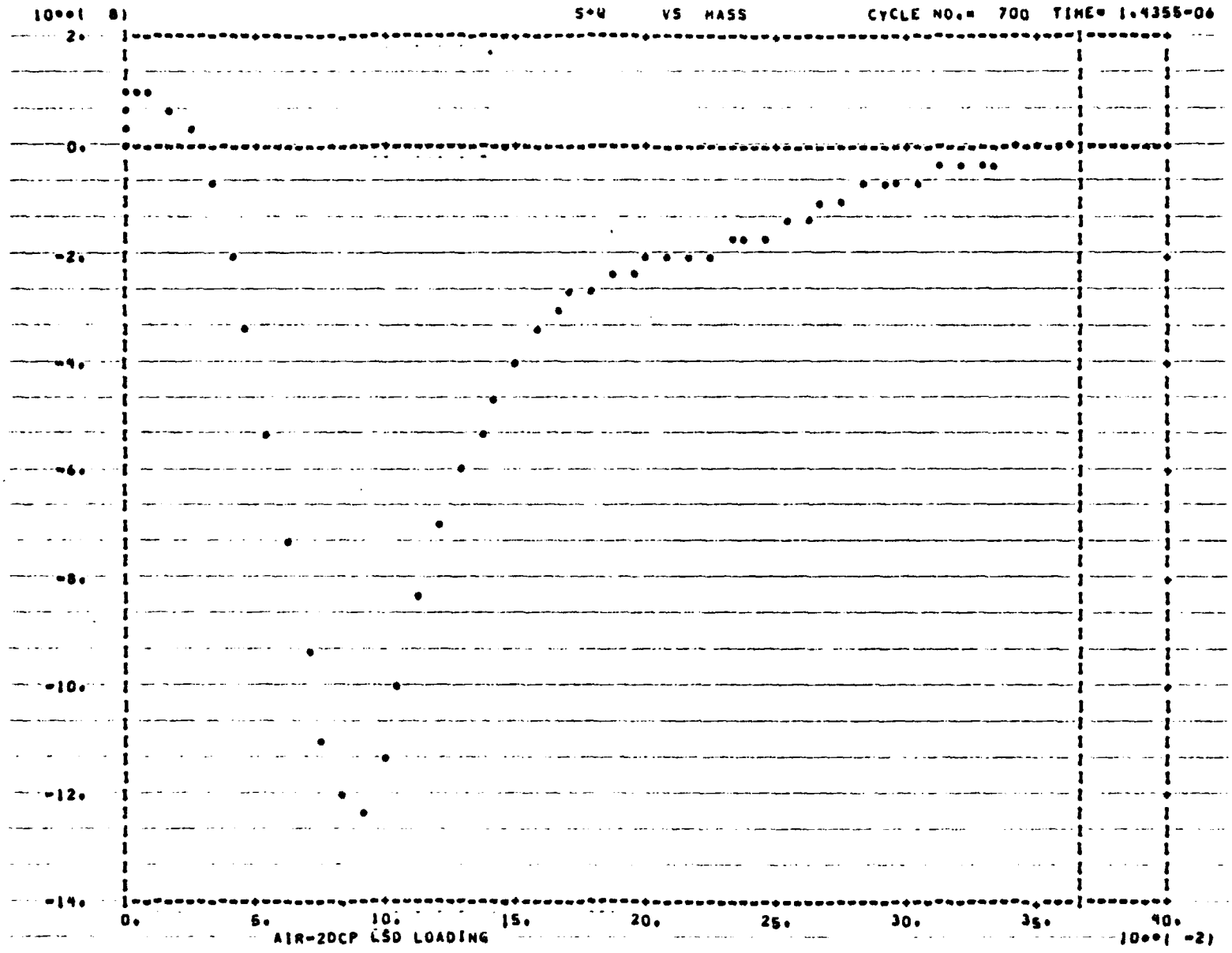

Figure 8. Stress (dynes/cm^2) versus mass depth (g/cm^2) at 1.44 μs.

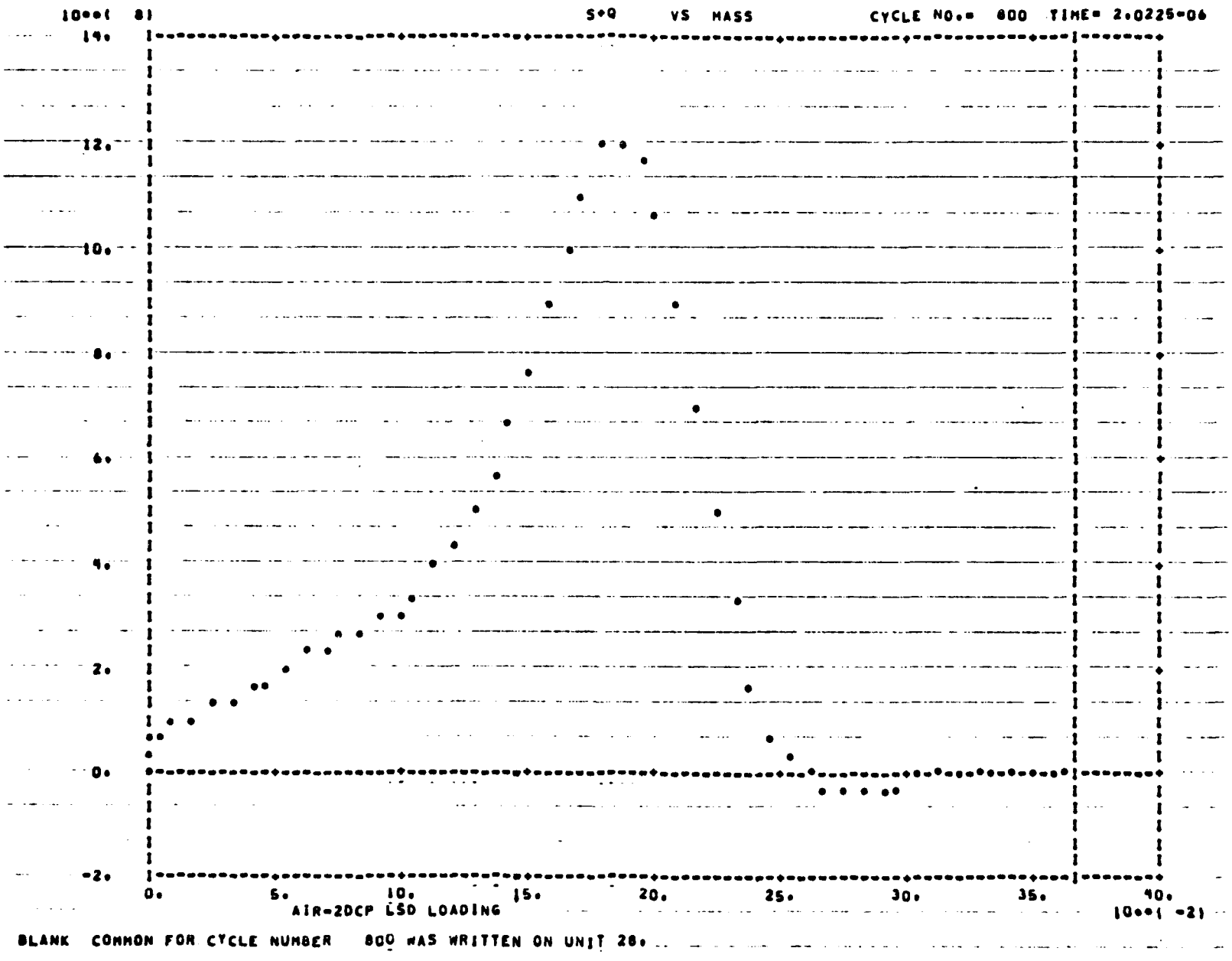

Figure 9. Stress (dynes/cm^2) versus mass depth (g/cm^2) at 2.02 μs.

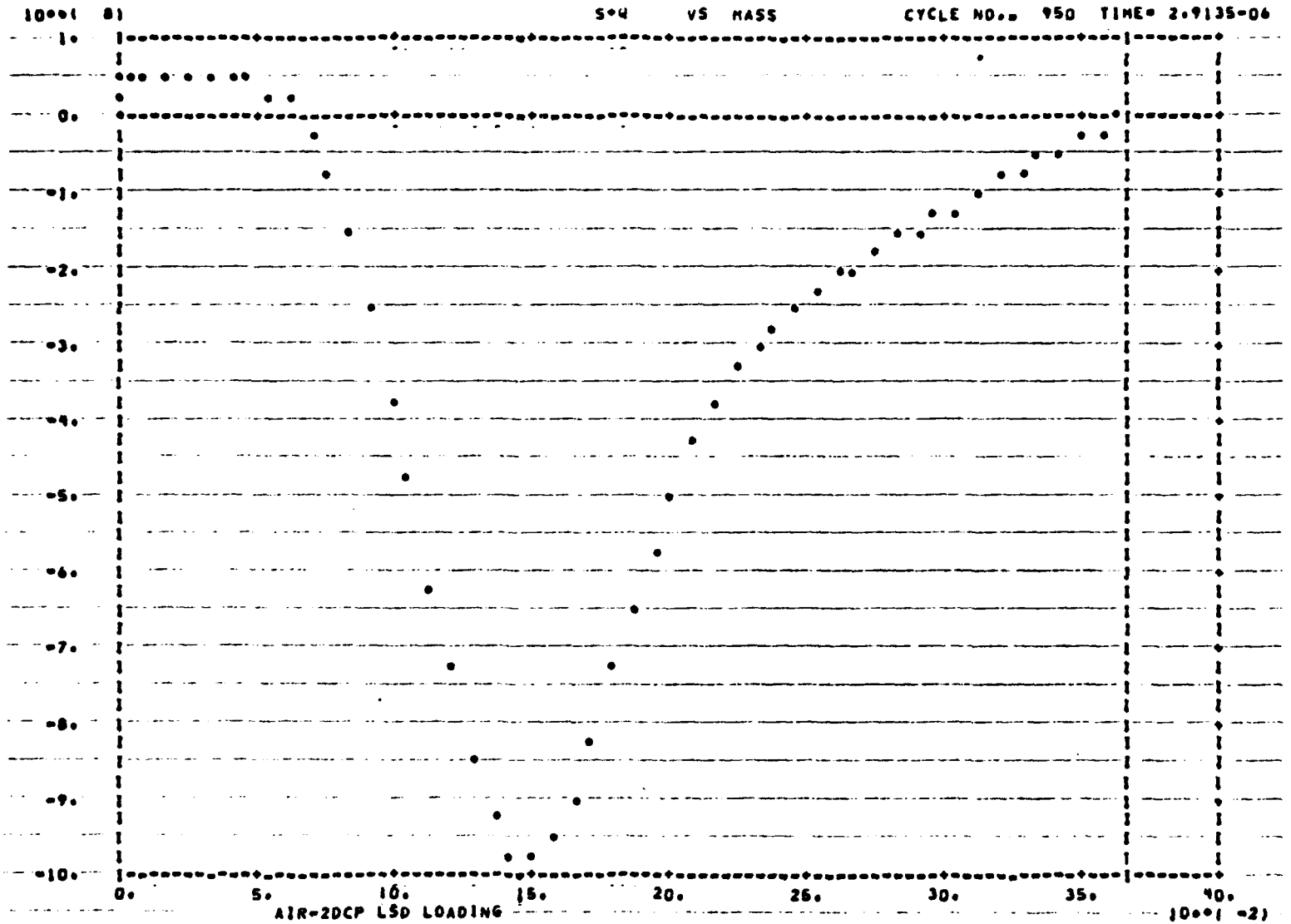

Figure 10. Stress (dynes/cm^2) versus mass depth (g/cm^2) at 2.91 μs.

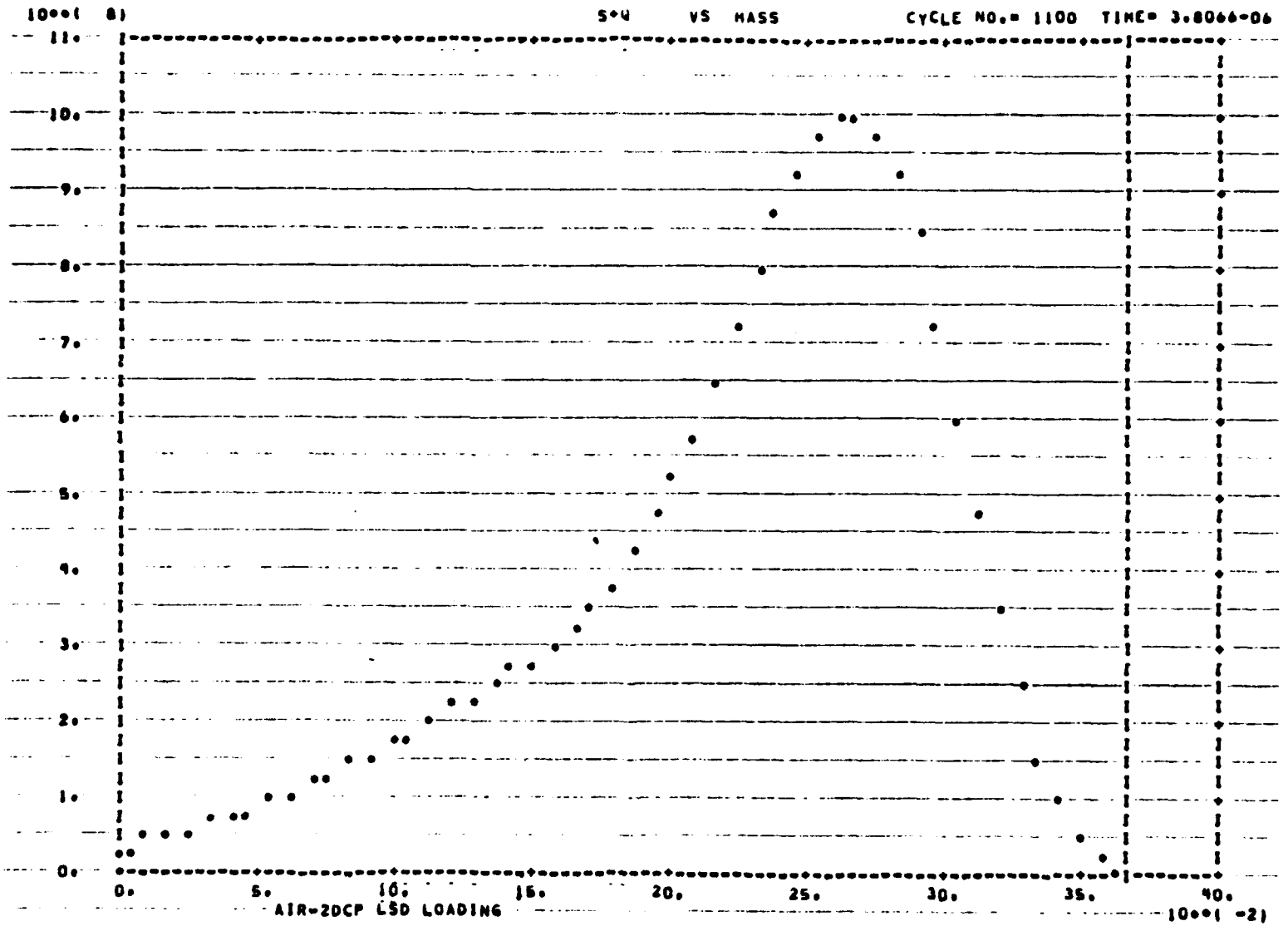

Figure 11. Stress (dynes/cm^2) versus mass depth (g/cm^2) at 3.81 μs.

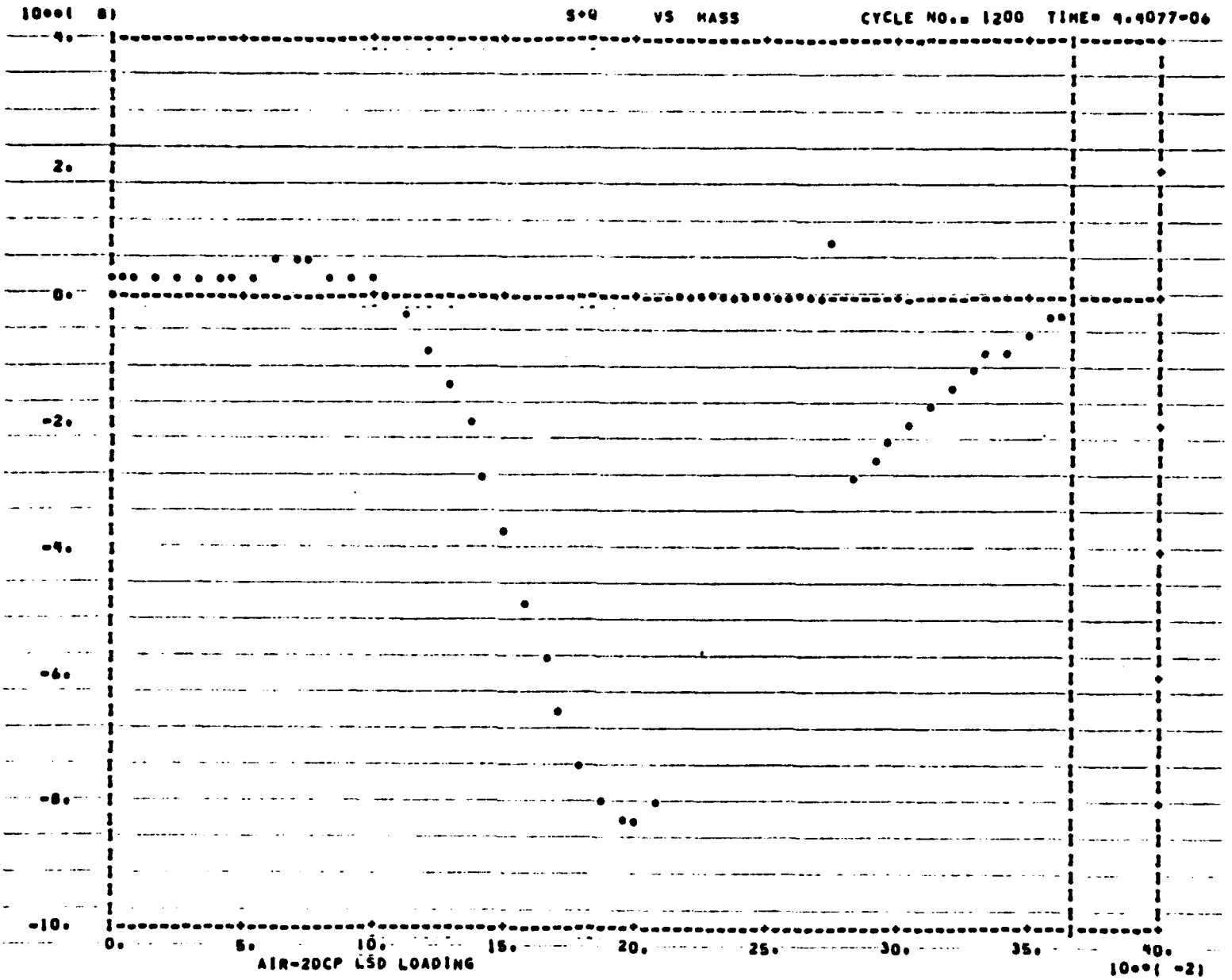

Figure 12. Stress (dynes/cm^2) versus mass depth (g/cm^2) at 4.41 μs.

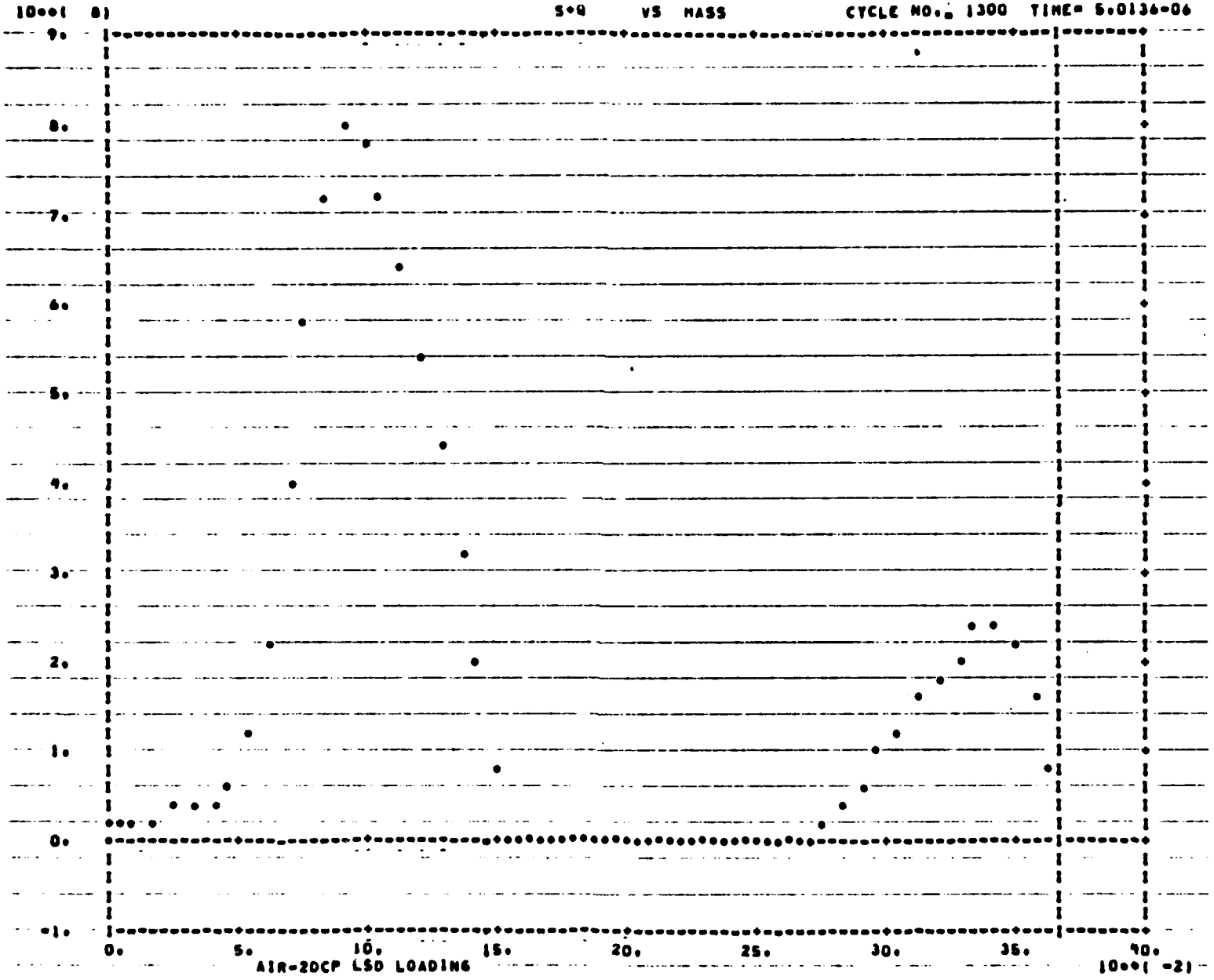

Figure 13. Stress (dynes/cm^2) versus mass depth (g/cm^2) at 5.01 μs.

6. CONCLUSIONS

The laser pulse chosen for the calculation described above, 100 joules/cm^2, in 10^{-8} seconds, is clearly well above the minimum required for fracture of the target. A lower fluence, a longer pulse time, or a thicker target would be required for an investigation of thresholds.

The calculation underlines the critical importance of void nucleation in damage processes described by the ductile fracture model we have used. Since void growth is exponential and, for this material, has a zero stress threshold, it might at first appear that almost any stress loading capable of nucleating cracks would automatically produce ultimate failure. A closer inspection of the behavior shows, however, that this is not true at lower stresses. Near the front and back surfaces, where wave overlap limits the magnitude of the tensile stress to values near threshold, the cracks grow very slowly. The fracture model near threshold is therefore dependent upon total impulse as well as upon peak stress. With repeated pulses, as remarked above, the required impulse could be supplied over a period of time.

The calculation did not assume initial porosity, since the empirical parameters used in the fracture model do not specify it, and arbitrarily inserting a porosity would therefore have been inconsistent. A refinement of the model is needed to represent initial defect distributions, which may strongly influence failure behavior.

Finally, the calculation demonstrates the effectiveness of high laser pulse intensity, in contrast to high fluence in producing damage, and provides a basis for further investigations of damage phenomena.

REFERENCES

1. Schriempf, J. T., "Response of Materials to Laser Radiation," NRL Report 7728, 1974.

2. Seaman, L., T. W. Barbee, Jr. and D. R. Curran, "Dynamic Fracture Criteria of Homogeneous Materials," Air Force Weapons Laboratory Report AFWL-TR-71-156, 1971.

3. Ireland, C. L. M., A. Yi, J. M. Aaron, and C. Grey Morgan, "Focal-Length Dependence of Air Breakdown by a 20-psec Laser Pulse," Appl. Phys. Letter 24, 175, 1974.

4. Shockey, D. A., L. Seaman, M. Austin, D. R. Curran, and R. A. Armistead (Stanford Research Institute), "Repetitively Pulsed Laser Induced Fracture as a Damage Enhancement Mechanism," Proceedings of the 1975 DOD Laser Effects/Hardening Conference, NASA TM X-73,084, Vol. II, p. 373.

5. Gurtman, G. A., M. H. Rice, R. A. Cecil and E. W. Sims, "Material Response Models for Radiation Effects on Advanced Three-Dimensional Composite Heat Shield Materials," Air Force Weapons Laboratory Report AFWL-TR-74-144, 1975.

6. White, J. W., "A New Form of Artificial Viscosity for Elastic Solids," J. Comp. Phys. 16, 119-126, 1974.

7. Triplett, J. R., and R. A. Cecil, "A Study of Laser-Supported Detonation Wave Interactions with Three-Dimensional Composites," Systems, Science and Software Report SSS-R-76-2743, 1 October 1975.